Stability and Structure of Telomeric DNA Sequences Forming Quadruplexes Containing Four G-Tetrads with Different Topological Arrangements†

Luigi Petraccone,‡ Eva Erra,‡ Veronica Esposito,§ Antonio Randazzo,§ Luciano Mayol,§ Lucia Nasti,‡ Guido Barone,‡ and Concetta Giancola*,‡

Dipartimento di Chimica, Via Cintia, Università "Federico II" di Napoli, 80126, Naples, Italy, and Dipartimento di Chimica delle Sostanze Naturali, Via Montesano, Università "Federico II" di Napoli, 80131, Naples, Italy

Received April 21, 2003; Revised Manuscript Received March 1, 2004

ABSTRACT: Telomeres are DNA−protein structures at the ends of eukaryotic chromosomes, the DNA of which comprise noncoding repeats of guanine-rich sequences. Telomeric DNA plays a fundamental role in protecting the cell from recombination and degradation. Telomeric sequences can form quadruplex structures stabilized by guanine quartets. These structures can be constructed from one, two, or four oligonucleotidic strands. Here, we report the thermodynamic characterization of the stability, analyzed by differential scanning calorimetry, of three DNA quadruplexes of different molecularity, all containing four G-tetrads. The conformational properties of these quadruple helices were studied by circular dichroism. The investigated oligomers form well-defined G-quadruplex structures in the presence of sodium ions. Two have the truncated telomeric sequence from *Oxytricha*, d(TGGGGT) and d(GGGGTTTTGGGG), which form a tetramolecular and bimolecular quadruplex, respectively. The third sequence, d(GGGGTTGGGGTGTGGGGTTGGGG) was designed to form a unimolecular quadruplex. The thermodynamic parameters of these quadruplexes have been determined. The tetramolecular structure is thermodynamically more stable than the bimolecular one, which, in turn, is more stable than the unimolecular one. The experimental data were discussed in light of the molecular-modeling study.

Telomeres, the end of chromosomes, contain guanine-rich DNA sequences. Telomeric DNA preserves chromosome ends from damage and recombination. Although most telomeric DNA is double-stranded, the extreme 3′ end of the telomere consists of single-stranded G-rich DNA overhangs (*1*, *2*). Structural studies (X-ray crystallographic and solution NMR[1] methods) have indicated that telomeric DNA sequences form a variety of quadruplex structures depending on the specific sequence, chain length, and presence of mono- and divalent cations (*3*−*6*). In all of these cases, the inter- or intramolecular quadruplex structures are stabilized by cyclic Hoogsteen hydrogen bonds of four guanines, called G-quartets or G-tetrads (*7*).

Telomerase is a ribonucleoprotein that adds repeating units of oligonucleotides to the 3′ ends of chromosomes (*1*, *8*), and its activity is highly correlated with tumorogenesis (*9*). The enhanced activity in the tumor cells is clearly related to the immortalization process (*10*). Consequently, telomerase inhibitors can be used as anticancer agents (*11*−*13*). One approach for inhibiting telomerase involves targeting the G-quadruplex DNA structures thought to be involved in telomere and telomerase function (*14*).

G-quadruplex structures have also been found in the aptamers against thrombin and HIV-1 integrase. These G-quadruplexes are able to inhibit thrombin and HIV-1 integrase activity, respectively (*15*−*17*). G-quadruplexes are thermodynamically stable although in some cases the quadruplex formation is kinetically controlled (for review, see ref *18*). Despite extensive investigations on the stability of G-quadruplexes (*6*, *18*−*21*), the influence of some factors (such as the molecularity of the complex, guanine number, role of cations) on the thermodynamic properties must be clarified.

In this paper, we report on a physicochemical characterization of three oligonucleotidic sequences, which in the presence of sodium ions assemble to form quadruplex structures at different molecularity, each containing four G-quartets. The first deoxynucleotide d(TGGGGT), from the 3′ overhang of *Oxytricha* telomere, forms a parallel-stranded quadruplex, $[d(TGGGGT)]_4$ (Figure 1A). The second oligonucleotide, d(GGGGTTTTGGGG), also deriving from the 3′ overhang of *Oxytricha* telomere, forms a complex containing two molecules, $[d(GGGGTTTTGGGG)]_2$ (*22*, *24*) (Figure 1B). The third sequence d(GGGGTTGGGGTGTGGGGTTGGGG) was designed to form a unimolecular quadruplex (*24*), very similar to that observed for the thrombin-binding aptamer (TBA) (*25*−*26*) (Figure 1C). In this paper, CD spectroscopy was used to confirm the conformational structure adopted by the oligomeric sequences. Differential scanning calorimetry (DSC) was performed to determine the

† This work was supported by a PRIN-MURST grant from the Italian "Ministero dell'Università e della Ricerca Scientifica e Tecnologica" (Rome).

* To whom correspondence should be addressed. Tel.: +39-081-674266. Fax: +39-081-674090. E-mail: giancola@chemistry.unina.it.

‡ Dipartimento di Chimica.

§ Dipartimento di Chimica delle Sostanze Naturali.

[1] Abbreviations: DSC, differential scanning calorimetry; G-tetrad, guanine quartet; G-quadruplex, guanine quadruplex; NMR, nuclear magnetic resonance; TBA, thrombin-binding aptamer; CD, circular dichroism; EDTA, ethylenediaminetetraacetic acid; HPLC, high-performance liquid chromatography.

10.1021/bi0300985 CCC: $27.50
Published on Web 04/01/2004

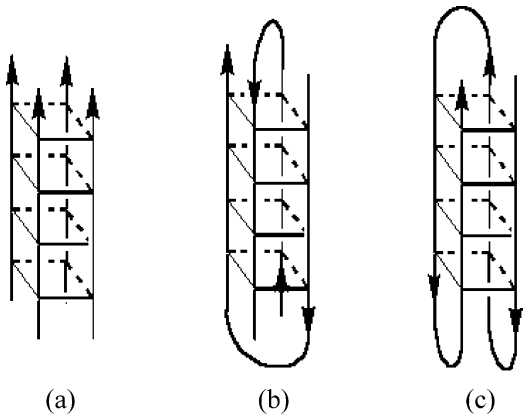

FIGURE 1: (a) Schematic structures of the parallel-stranded tetramolecular quadruplex $[d(TGGGGT)]_4$, (b) antiparallel folded-back bimolecular quadruplex $[d(GGGGTTTTGGGG)]_2$, and (c) folded-back unimolecular quadruplex d(GGGGTTGGGGTGTGGGGTTGGGG).

stability and the melting behavior of the DNA quadruplexes, thereby providing a complete thermodynamic characterization of DNA quadruple-helical structures. Molecular modeling was used to compare the quadruplex structures and to examine them in light of the existing experimental data.

MATERIALS AND METHODS

Substances. The oligonucleotides d(TGGGGT), d(GGGGTTTTGGGG), and d(GGGGTTGGGGTGTGGGGTTGGGG) were synthesized by the β-cyanoethylphosphoramidite method on a Millipore Cyclon Plus DNA synthesizer and purified by a HPLC Waters 515, followed by desalting on Sep-pak C18 columns. DNA quadruplexes were formed by dissolving solid lyophilized oligonucleotide in the appropriate buffer and were annealed by heating to 90 °C for 5 min and slow cooling to room temperature. The solutions were equilibrated at 4 °C for 1 day before performing the experiments. The buffer consisting of 10 mM sodium phosphate, 200 mM NaCl, and 0.1 mM EDTA was used. d(TGGGGT), d(GGGGTTTTGGGG), and d(GGGGTTGGGGTGTGGGGTTGGGG) concentrations were determined from their adsorption measured at 90 °C, in the same buffer, using molar extinction coefficients $\epsilon(260\ nm) = 57\ 800\ M^{-1}\ cm^{-1}$, $121\ 200\ M^{-1}\ cm^{-1}$, and $228\ 099\ M^{-1}\ cm^{-1}$, respectively. The molar extinction coefficients were calculated by the nearest neighbor model (*27*).

CD Spectroscopy. The conformation of the quadruplexes was derived by inspection of their CD spectra. The spectra were obtained on a JASCO 715 CD spectrophotometer equipped with a programmable, thermoelectrically controlled cell holder (JASCO PTC-348). The wavelength was varied from 200 to 340 nm at 10 nm min^{-1}. The measurements were made at 20 °C, using a square quarts cell with a 0.1 cm path length. The molar ellipticity was calculated from the equation $[\vartheta] = 100\vartheta/cl$, where ϑ is the ellipticity value, c is the concentration of the quadruplex, and l is the path length of the cell in centimeters. CD spectra were recorded with a response of 8 s, at a 2.0 nm bandwidth. The sample spectra were subtracted by the buffer spectrum. Each spectrum reported is an average of at least three scans.

DSC. Differential scanning measurements were performed on a second generation Setaram Micro-DSC. The energy of dissociation/unfolding processes is measured in power units, with the raw output data expressed as power units versus temperature. The power units are converted into apparent molar heat capacity, ΔC_P^0, in J mol^{-1} K^{-1}, using the equation

$$\Delta C_P^0 = \frac{P}{\sigma m}$$

where P is power in J s^{-1}, σ is the scan rate in K s^{-1}, and m is the number of moles of quadruplex in the sample. The instrument was interfaced to an IBM PC computer for automatic data collection and analysis using the software previously described (*28*). The excess molar heat capacity function $\langle \Delta C_P^0 \rangle$ was obtained after a baseline subtraction, assuming that the baseline is given by the linear temperature dependence of the native-state heat capacity (*29*). A buffer versus buffer scan was subtracted from the sample scan. All systems were tested for reversibility by running heating and cooling curves at the same scan rate (in the range of 0.3−1 °C min^{-1}). The process enthalpies, $\Delta H°(T_m)$, were obtained by integrating the area under the heat capacity versus the temperature curves; T_m is the temperature corresponding to the maximum of each DSC peak. The thermodynamic parameters in Table 1 represent averages of heating curves from three to five experiments. The reported errors for thermodynamic parameters are the standard deviations of the mean from the multiple determinations.

Modeling Study. Complete structural and modeling studies are reported in the literature for the tetra- and bimolecular quadruplexes (*22*−*24*, *30*−*34*), while the only existing NMR data for the d(GGGGTTGGGGTGTGGGGTTGGGG) sequence are recently reported by some of us (*24*). To built this quadruplex, it was first generated from the four G-tetrads by using the coordinates of the dG residues in the crystal structure of the d(GGGGTTTTGGGG) reported by Kang et al. (*35*). Indeed, in this quadruplex, each quartet has its guanines in a G(*syn*)-G(*anti*)-G(*syn*)-G(*anti*) arrangement and each strand has only an antiparallel neighbor, which the previously reported NMR study suggests for the d(GGGGTTGGGGTGTGGGGTTGGGG) sequence (*24*). Then, the TT loops and the TGT loop were added to the four G-tetrads to obtain the final unimolecular chair-type structure. The resulting coordinates of the quadruplex were energy-minimized in a vacuum for 200 steps of the steepest descent method keeping the four G-tetrads fixed in position, allowing only the loops to relax.

Three internal sodium ions were positioned in the central channel to allow coordination for each sodium ion, with the four carbonyl oxygen atoms of the two adjacent G-quartets completing the octahedral coordination sphere. The remaining sodium counterions were added to give electrical neutrality and then the neutralized system was solvated with a 40 × 40 × 40 Å box of Monte Carlo TIP3P water (*36*), with periodic boundary conditions. The water molecules that were nearest to 2.6 Å from any of the solute atoms were removed. The Amber force field was utilized (*37*). The solvated system was minimized using 1000 steps of the steepest descent method followed by the conjugate method until the convergence to a root-mean-square gradient of 0.1 kcal mol^{-1} $Å^{-1}$.

For comparative purposes, the structures of the $[d(GGGGTTTTGGGG)]_2$ and $[d(TGGGGT)]_4$ quadruplexes were

Table 1: Thermodynamic Parameters for the Dissociation/Unfolding of the Three Quadruplexes

quadruplex	T_m (°C)	$\Delta H°(T_m)$ (kJ mol^{-1})	$\Delta S°(T_m)$ (kJ mol^{-1} K^{-1})	$\Delta G°$(298 K) (kJ mol^{-1})
[d(TGGGGT)]$_4$	74.6 ± 0.2	320 ± 8	0.73 ± 0.04	102.5 ± 2.6
[d(GGGGTTTTGGGG)]$_2$	47.0 ± 0.2[a]	100 ± 11	0.31 ± 0.03	7.6 ± 0.6
	66.6 ± 0.2[b]	340 ± 22	1.00 ± 0.03	42.0 ± 7.2
d(GGGGTTGGGGTGTGGGGTTGGGG)	86.0 ± 0.2	209 ± 10	0.58 ± 0.02	36.2 ± 2.9

[a] Premelting process: $A_2^* \leftrightarrows A_2$. [b] Dissociation process: $A_2 \leftrightarrows 2A$.

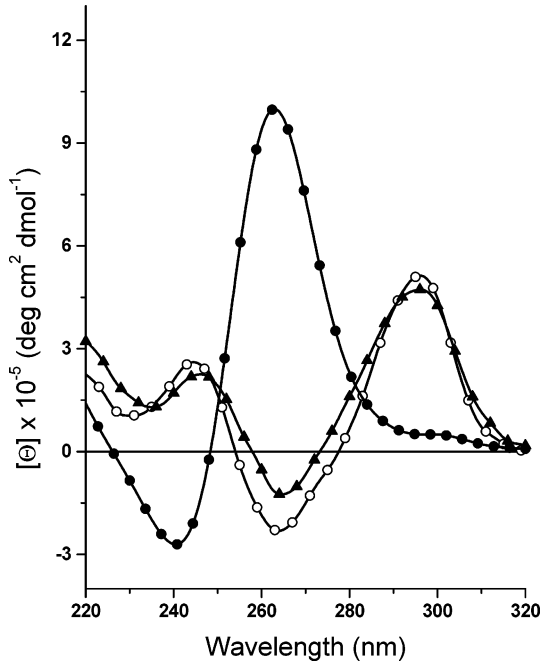

FIGURE 2: CD spectra at 20 °C of tetramolecular (●), bimolecular (▲), and unimolecular (○) quadruplexes.

also built by using the coordinates of the previously reported structures (*22*, *31*), and the corresponding solvated systems were minimized with the same protocol described above. For the [d(TGGGGT)]$_4$ quadruplex, both the 3′- and 5′-terminal thymine residues, which do not participate in the quadruplex motif, were omitted (*32*).

RESULTS

CD Studies. Figure 2 shows the CD spectra of the three oligonucleotides at pH 7.0, $T = 20$ °C, and $C = 5 \times 10^{-6}$ M. The spectrum of d(TGGGGT) is distinctly different from the spectra of d(GGGGTTTTGGGG) and d(GGGGTTGGGGTGTGGGGTTGGGG). The former exhibits a strong positive band at 263 nm and a negative band at 241 nm. It corresponds to that assigned to the parallel-stranded quadruplex formed from four strands of d(TGGGGT) (*38* and references therein, *39*). The spectra of d(GGGGTTTTGGGG) and d(GGGGTTGGGGTGTGGGGTTGGGG) are similar to each other, and signature bands for antiparallel quadruplexes were observed, a negative band at 263 nm and a positive band at 295 nm. The spectrum for the d(GGGGTTTTGGGG) corresponds to that assigned to the quadruplex formed by dimerizing two hairpins, while the spectrum for the d(GGGGTTGGGGTGTGGGGTTGGGG) is identical to that for the unimolecular quadruplex formed from the folding of one strand (*6*, *40*−*42*).

Thermodynamic Behavior. We have investigated the unfolding of the quadruplexes using microcalorimetry. The first step of our study was to determine the molecularity of each quadruplex at the buffer and concentration conditions used for DSC studies. Thus, all three samples were analyzed by ^{1}H NMR. The structures of [d(TGGGGT)]$_4$ and [d(GGGGTTTTGGGG)]$_2$ have been already characterized by NMR (*22*−*24*, *30*−*31*). Both complexes were easily prepared (see the Materials and Methods), and their one-dimensional proton spectra clearly showed that a single, well-defined complex is plainly observable in solution, thus suggesting the absence of conformational heterogeneity. Two-dimensional nuclear Overhauser effect spectrometry (NOESY) spectra show very characteristic nuclear Overhauser effect (NOE) connectivities that are consistent with the structure reported in the literature. Hence, the NMR data confirm that d(TGGGGT) and d(GGGGTTTTGGGG) form tetra- and bimolecular complexes, respectively. In particular, [d(TGGGGT)]$_4$ is characterized by four grooves of identical medium width and all nucleotides in the anti conformation, whereas [d(GGGGTTTTGGGG)]$_2$ is characterized by four G-tetrads with guanosines that adopt the *syn-syn-anti-anti* conformations. Each tetrad stacks upon the other, so that consecutive Gs in each DNA strand adopt an alterning 5′-3′-*syn-anti* relationship. Consequently, this quadruplex is characterized by two medium, one wide, and one narrow groove between strands. Concerning d(GGGGTTGGGGTGTGGGGTTGGGG), its NMR study was already reported by some of us (*24*) by using a potassium buffer. To confirm the molecularity of this quadruplex in the presence of Na^+, we repeated an in-depth structural study. As for d(TGGGGT) and d(GGGGTTTTGGGG), despite the high number of Gs present in the sequence, one-dimensional ^{1}H NMR spectrum of d(GGGGTTGGGGTGTGGGGTTGGGG) shows that a single, well-defined complex is plainly observable in solution, thus indicating that the oligomer forms 100% the expected complex. All of the resulting resonances were extremely similar to those observed for the same molecule in K^+. Although the observed number of resonances would also be consistent with a symmetrical four-stranded parallel quadruplex, the line widths of the nonexchangeable resonances (<10 Hz) are only compatible with a low molecular weight, thus being indicative of a unimolecular-folded species. Further, NOESY data demostrate that eight guanosines are in a syn conformation because the G-H8/H1′ intraresidue NOEs of these residues are very strong. This is in perfect agreement with a quadruplex structure formed by antiparallel strands (*25*, *26*). Moreover, the CD spectrum of d(GGGGTTGGGGTGTGGGGTTGGGG) is typical of folded quadruplexes involving deoxyguanosine alternating between syn and anti conformations about the glycosidic bond, exhibiting a maximum at 293 nm and a minimum at 265 nm. Therefore, the whole data suggest that d(GGGGTTGGGGTGTGGGGTTGGGG) is a unimolecular quadruplex, whose structure is

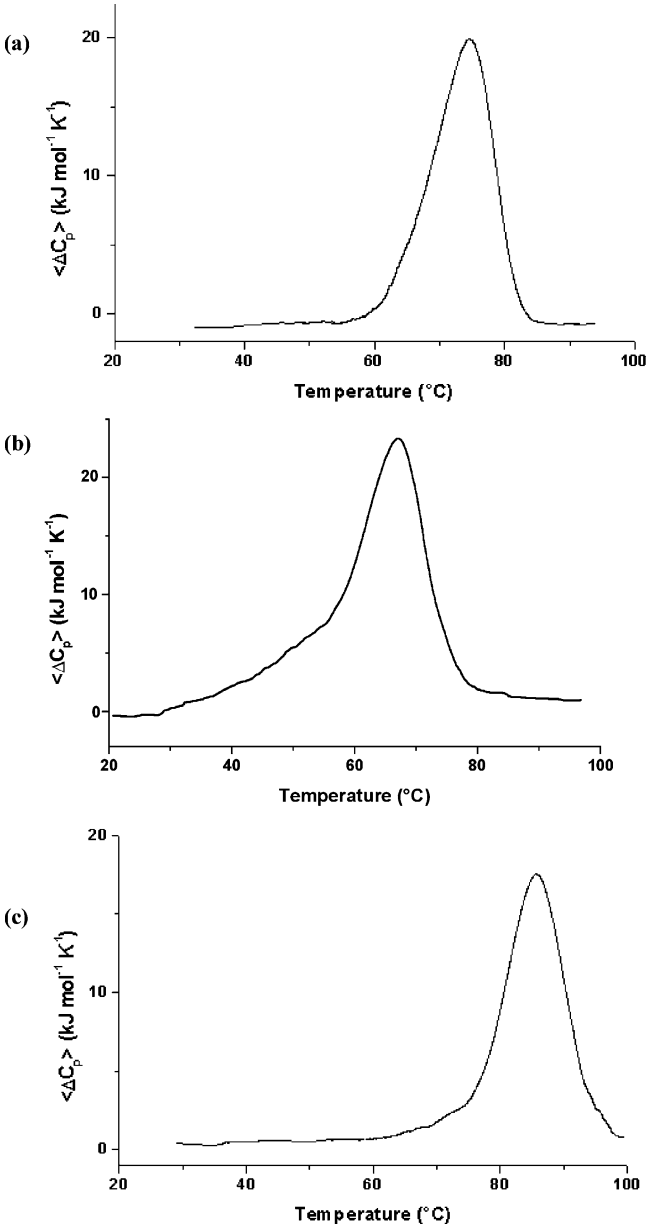

FIGURE 3: Excess heat capacity versus temperature profiles for (a) tetramolecular, (b) bimolecular, and (c) unimolecular quadruplexes.

basically superimposable to that observed in the presence of K^+ and similar to that possessed by thrombin-binding aptamer (TBA) (*25*−*26*), with four G-tetrads formed from guanosines of alternating anti-syn-anti-syn conformation and with each *syn*-guanosine donating hydrogen bonds to an adjacent *anti*-guanosine and accepting hydrogen bonds from the other adjacent guanosine.

The DSC melting profiles are shown in Figure 3. The comparison of the calorimetric profiles of these quadruplexes at different molecularity is a suitable method to extract the energetic contributions of the G-tetrads in structures with different topological arrangements. All of the measurements were performed at the constant quadruplex concentration (1.6×10^{-4} M) because the dissociation of the complexes of molecularity greater than one result in a concentration dependence of the thermodynamic parameters (*43*). In the selected conditions, the dissociation/unfolding process is highly reversible, as demonstrated by the recovery of the original signal by rescanning the same sample. Furthermore, the change of the heating rate from 0.3 to 1 °C min^{-1} does not alter the thermodynamic parameters significantly, thereby demonstrating that the studied processes are not kinetically determined. Hence, the dissociation and formation rates of the complexes are equal at any temperature; i.e., the equilibrium was achieved. The Gibbs energy value at 298 K can be calculated by the experimental thermodynamic parameters. $\Delta G°$ values are a rigorous measurement of the thermodynamic stability. Thermodynamic parameters obtained by DSC curves are listed in Table 1. The calorimetric profiles of each quadruplex present some peculiarities. The calorimetric curve of $[d(TGGGGT)]_4$ shows a symmetric shape with a maximum centered to 74.6 °C (Figure 3A). The dissociation process can be described by a two-state mechanism in

Scheme 1

$$A_4 \leftrightarrows 4A$$

where A_4 represents the quadruplex complex and A is the single strand.

The $\Delta H°(T_m)$ value is 320 kJ mol^{-1}, corresponding to a value of 80 kJ mol^{-1} per tetrad, in good agreement with the value of 77 kJ mol^{-1} found by us for the $[d(TGGGT)]_4$ quadruplex (*39*) and by other authors for different quadruplexes (*5*, *42*, *44*). The entropy change, $\Delta S°(T_m)$, was determined from integrating the curve obtained by dividing the heat capacity curve by the absolute temperature, i.e., $\Delta S°(T_m) = \int_{T_i}^{T_f}(\Delta C_p/T)\, dT$.

The $\Delta G°$ value was calculated at 298 K from the relationship $\Delta G°(298) = \Delta H°(T_m) - 298\Delta S°(T_m)$, assuming a negligible difference in the heat capacity between the initial and final states. $\Delta G°(298)$ is 102.5 kJ mol^{-1}. This value reveals that the $[d(TGGGGT)]_4$ exhibits considerable stability at 298 K and each G-tetrad contributes to the stability with 25.6 kJ mol^{-1}.

The bimolecular complex, $[d(GGGGTTTTGGGG)]_2$, dissociates in a biphasic transition, as indicated by the presence of an additional small peak as a shoulder at a lower temperature (Figure 3B). On the other hand, as previously cited, ^1H NMR measurements performed in the same solution conditions of calorimetric experiments show that a single, well-defined species is plainly observable in solution. The dimer adopts a symmetric hairpin structure, where the planes of the two thymine loops are mutually perpendicular (*22*). Hence, the presence of a biphasic calorimetric profile is not imputable to different topological arrangements. It is possible to rationalize these observations supposing that the experimental curve can be represented as the sum of two sequential two-state transitions, an intramolecular premelting event followed by a melting transition, according to

Scheme 2

$$A_2^* \leftrightarrows A_2 \leftrightarrows 2A$$

where A_2^* and A_2 represent two different states of quadruplex and A represents the single strand. The experimental calorimetric curves were analyzed using a deconvolution procedure (see the Appendix), which assumes the overall melting to be composed of two sequential two-state transitions with ΔC_p for the overall transition being equal to zero.

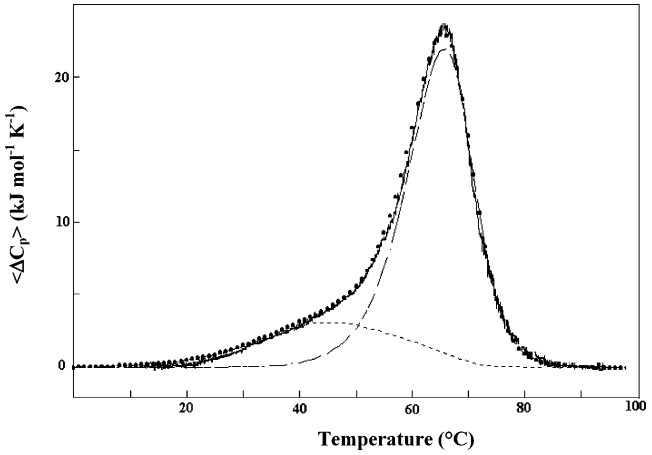

FIGURE 4: Excess heat capacity of the bimolecular quadruplex. (—) Experimental data, (●) total simulated transition, and (— — —) and (- · - · -) deconvolution in two transitions.

Figure 4 shows the good agreement between the experimental curve and that simulated on the basis of Scheme 2. The thermodynamic parameters obtained by the deconvolution procedure are listed in Table 1. The low-temperature peak, centered at 47.0 °C, is attributable to the $A_2^* \leftrightarrows A_2$ process, while the high-temperature peak, centered to 66.6 °C, is due to the dissociation of the quadruplex structure in two single strands. The two sequential processes contribute to the total enthalpy with 100 and 340 kJ mol^{-1}, respectively. The total $\Delta G°(298)$ is 49.6 kJ mol^{-1}, about half of the value found for the tetramolecular quadruplex.

Finally, the unimolecular quadruplex, d(GGGGTTGGGGTGTGGGGTTGGGG), exhibits the highest melting temperature at 86.0 °C (Figure 3C). The unfolding process follows a two-state mechanism, and the integration of the denaturation peak gives a $\Delta H°(T_m)$ of 209 kJ mol^{-1}, a lower value than that of the tetra- and bimolecular quadruplexes. The $\Delta G°(298)$ value is 36.2 kJ mol^{-1} and reveals that the unimolecular quadruplex is the thermodynamically least-stable quadruplex.

Molecular Modeling. Molecular modeling was used to compare the structure of the studied quadruplexes. The molecular model of the unimolecular quadruplex is shown in Figure 5 in comparison with the models of the bi- and tetramolecular complexes. In all of the minimized structures, there is a slight displacement of the internal sodium ions from the center of the consecutive quartets, which is attributable to the effect of the electrostatic repulsion. In the unimolecular quadruplex, the thymines at the 3′ end of the short T_2 loops are completely exposed toward the solvent and do not stack over the neighboring G-quartet, while the thymine residues in the TGT loop stack on the adjacent guanine residues involved in the G-tetrad. On the other hand, the thymine residues in the T_4 loops of the bimolecular quadruplex are highly structured, forming hydrogen bonds and stacking interactions also reported in a previous study (*32*). The different glycosidic bond conformation of the guanosine residues and the different strand orientation for the three quadruplexes bring nonequivalent G-tetrads. In particular, it can be noted that the degree of coplanarity between the dG residues in each G-tetrad is greater in the tetra- and bimolecular quadruplexes than that in the unimolecular one. It is important to underline that the perturbation of each G-tetrad directly affects the stacking energy of the neighboring G-tetrad. Furthermore, analysis of the hydrogen-bond scheme inside the G-tetrads reveals that, in the tetramolecular and bimolecular complexes, each G-tetrad shows the same hydrogen-bond scheme with an optimum distance and angle between the donor and acceptor atoms resulting in a strong hydrogen bond. Indeed in the unimolecolar quadruplex, there is a change in the direction of hydrogen-bond donors and acceptors between adjacent quartets, with a weakness in the hydrogen bonds compared to the tetra- and bimolecular quadruplexes.

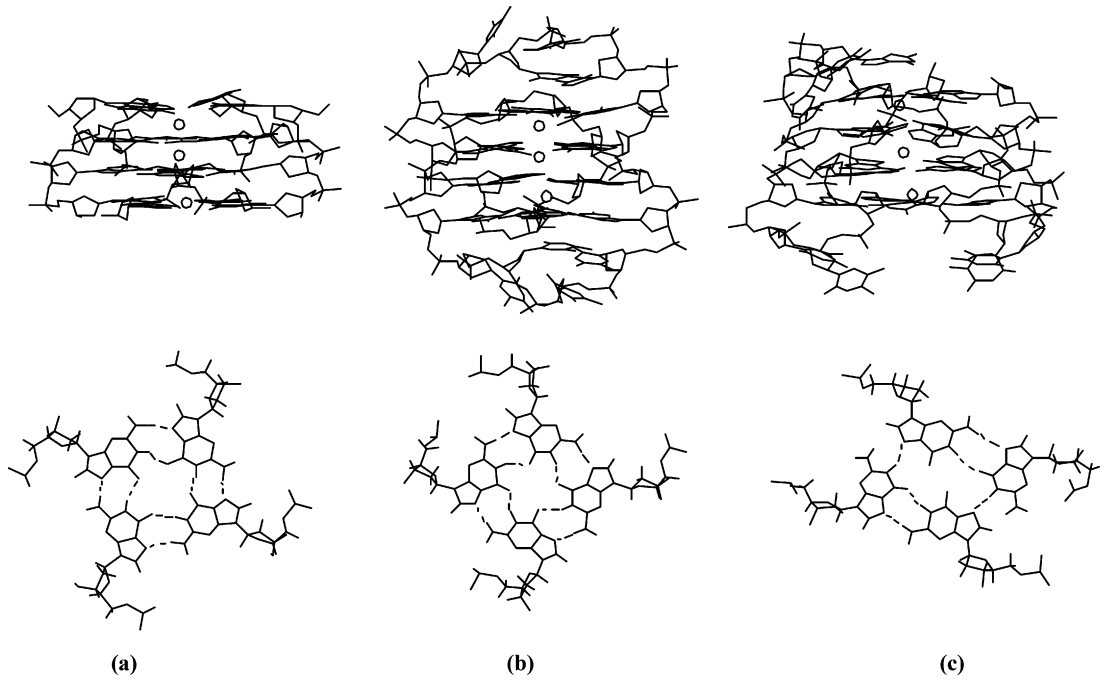

FIGURE 5: Structures of (a) tetramolecular, (b) bimolecular, and (c) unimolecular quadruplexes generated by molecular mechanics. The internal sodium ions are shown as open circles. At the bottom the structure of the G-tetrad, adjacent to the T_2 loop, the unimolecular quadruplex (c) is compared to the characteristic G-tetrad of the tetra- (a) and bimolecular (b) quadruplexes.

DISCUSSION

We have examined the thermodynamic stability of three quadruplexes, each containing four G-tetrads. NMR and CD measurements show that the investigated sequences, d(TGGGGT), d(GGGGTTTTGGGG), and d(GGGGTTGGGGTGTGGGGTTGGGG), assemble to form tetra-, bi-, and unimolecular quadruple helices, respectively. The thermodynamic stability of the quadruplexes was investigated by DSC following their dissociation/denaturation process. Because the process was found reversible for all the quadruplexes, equilibrium thermodynamic laws were applied and $\Delta G°$ values at 298 K were calculated. The $\Delta G°$ values were calculated with the assumption that there is no difference in the heat capacity between the initial and final states, as commonly accepted (*43*−*47*).

Inspection of Table 1 reveals that the unimolecular quadruplex melts at a higher temperature than the bi- and tetramolecular quadruplexes. The melting temperatures do not reflect the thermodynamic stability trend, based on the Gibbs energy values, which follows the order: tetramolecular > bimolecular > unimolecular. This order is also retained when the quadruplex concentration is decreased from 160 to 1 μM.

DSC data for the $[d(GGGGTTTTGGGG)]_2$ quadruplex reveal a two-step dissociation. The good agreement between the experimental and deconvoluted curves demonstrates that the experimental curve can be reproduced by the sum of two sequential two-state transitions. The deconvolution protocol (described in the Appendix) allowed us to characterize each of the two-step transitions. The first process is probably attributable to a conformational change in the T_4 loop. This hypothesis is reinforced by the results of the molecular mechanics calculations showing that the thymine residues are arranged in four-nucleotide loops and are capable of forming hydrogen bonds and stacking interactions, which stabilize the quadruplex structure, as already reported in the literature (*32*). The deconvolution analysis allowed us to assign to this intramolecular transition, centered at 48.0 °C, an enthalpy value of 100 kJ mol^{-1}. On the other hand, the $\Delta H°$ value for the dissociation/unfolding process, subtracted by the loops contribution, is 340 kJ mol^{-1} (85 kJ mol^{-1} per tetrad) in good agreement with the value of 320 kJ mol^{-1} (80 kJ mol^{-1}), found for the tetramolecular quadruplex. It can be underlined that for both tetra- and bimolecular quadruplexes the $\Delta H°$ values per quartet are in perfect agreement with previously reported values on other quadruplexes (*5*, *39*, *48*). Instead, the $\Delta G°$ value per quartet for the tetramolecular quadruplex is higher (25 kJ mol^{-1}) than that for the bimolecular quadruplex (10.5 kJ mol^{-1}). The higher thermodynamic stability of $[d(TGGGT)]_4$ is due to the lower entropic contribution to the dissociation process. The higher entropic contribution in the dissociation/unfolding process determined for the bimolecular complex, which cannot simply be explained on the basis of molecularity, suggests more rigid structures with respect to that of the tetramolecular complex. This is probably due to the presence of the two "structured" T_4 loops at the ends that force the G-quartets in more rigid positions.

With regard to a previous DSC study on the d(GGGGTTTTGGGG) sequence (*40*), our thermodynamic parameters are in sufficient agreement. The substantial difference is that in their paper the authors analyze the calorimetric profile as a single-step transition, although they declare that "formation of tetraplex is very nearly a fully cooperative reaction, with only minor populations of any intermediates". Our analysis shows that a one-step transition interpretation of the calorimetric profile is insufficient.

A rather unexpected finding is that the unimolecular quadruplex is the least stable among the studied quadruplexes, as shown by the $\Delta G°$ value. It should be noted that the high melting temperature is due to the entropic term that is the lowest among the studied systems. In the case of the unimolecular quadruplex, the presence of short loops does not produce a premelting transition but reduces the thermodynamic stability, making the enthalpic term less favorable at 209 kJ mol^{-1}, i.e., 52 kJ mol^{-1} per tetrad, a value remarkably lower than the values found and commented on above. The $\Delta G°$ value per tetrad is 9 kJ mol^{-1}. Hence, the lowest stability among the three quadruplexes is mainly due to the enthalpic term. Molecular modeling reveals that in the unimolecular quadruplex the coplanarity between the dG residues in each G-tetrad is partially lost, which results in a weakening of hydrogen bonds and stacking interactions compared to the tetra- and bimolecular quadruplexes. In particular, in the tetrad formed by the guanine residues, linked by −TT− loops, two hydrogen bonds are completely lost (bottom of Figure 5C). These findings reflect the steric effects involved in the two short −TT− loops in comparison with the longer −TTTT− loops of the bimolecular complex and could justify the lower enthalpy observed for the dissociation/unfolding of the unimolecular quadruplex (*42*). In fact, a calorimetric value of 107 kJ mol^{-1}, corresponding to 53 kJ mol^{-1} per tetrad, was reported for the thrombin aptamer that contains two G-quartets and includes two −TT− loops (*6*). In conclusion, the detailed analysis of enthalpic and entropic contributions for the dissociation/unfolding processes of the three quadruplexes, all containing four G-tetrads, shows that the tetramolecular complex is the most stable among the studied systems.

DNA quadruplex structures have been implicated in many biological processes. They are involved in telomeric DNA structure and telomerase inhibition and may exert a biological role in several different ways depending on the particular quadruplex topology. For example, alignment of certain sequences on separate duplexes, necessary for recombinational events, may be facilitated by parallel quadruplex formation. The formation of a folded quadruplex in a gene promoter region may be important for gene activation in vivo (*49*). A detailed thermodynamic study is the first step in determining what type of the possible different stable structures will be formed by the G-rich strand depending on the molecularity, the G-tetrad conformation, and the presence and length of the loops. It provide more insight into the factors that govern the interconversion processes between different topological motifs.

APPENDIX

The global unfolding/dissociation process for $[d(GGGGTTTTGGGG)]_2$ can be represented as the sum of two sequential two-state transitions, an intramolecular premelting event followed by a melting transition, according to the following scheme:

$$A_2^* \overset{K_1}{\rightleftharpoons} A_2 \overset{K_2}{\rightleftharpoons} 2A$$

where A_2^* and A_2 represent two different states of the quadruplex and A represents the single strand. Considering the stoichiometry and conservation of mass, the following equations hold at any temperature:

$$C_t = C_{A_2^*} + C_{A_2} + \frac{1}{2}C_A \quad (1)$$

where C_t is the molar concentration of the quadruplex. The equilibrium constants K_1 and K_2 are

$$K_1 = \frac{[A_2]}{[A_2^*]} \quad (2)$$

$$K_2 = \frac{[A]^2}{[A_2]} \quad (3)$$

The fractional population of each species can be defined as

$$f_x = \frac{C_x}{C_t} \quad (4)$$

where x represents A_2^*, A_2, and A. We can recast the above equations as

$$f_{A_2^*} + f_{A_2} + \frac{1}{2}f_A = 1 \quad (5)$$

$$K_1 = \frac{f_A}{f_{A_2^*}} \quad (6)$$

$$K_2 = \frac{f_A^2}{f_{A_2}}C_t \quad (7)$$

The eqs 5−7 describe the set of sequential reactions. Their solution permits the determination of the excess enthalpy $\langle \Delta H \rangle$ of this system according to the equation

$$\langle \Delta H \rangle = (1 - f_{A_2^*})\Delta H_1 + \frac{1}{2}f_A \Delta H_2 \quad (8)$$

where ΔH_1 and ΔH_2 are the enthalpy changes of the two sequential transitions.

The corresponding excess heat capacity, $\langle \Delta C_p \rangle$, can be calculated by the numerical differentiation of eq 8

$$\langle \Delta C_p \rangle = \frac{\partial \langle \Delta H \rangle}{\partial T} \quad (9)$$

At any temperature, the equilibrium constants have been determined according to the equation

$$K_i = K_i(T_{mi})\, e^{(-(\Delta H_i/R))((1/T)-(1/T_{mi}))} \quad (10)$$

where we assumed that the values of $K_1(T_{m_1})$ and $K_2(T_{m_2})$ are 1 and $C_t/2$, respectively.

REFERENCES

1. Blackburn, E. H. (1991) Structure and function of telomeres, *Nature 350*, 569−573.
2. Rhodes, D., and Giraldo, R. (1995) Telomere structure and function, *Curr. Opin. Struct. Biol. 5*, 311−322.
3. Hud, N. V., Smith, F. W., Anet, F. A., and Feigon, J. (1996) The selectivity for K^+ versus Na^+ in DNA quadruplexes is dominated by relative free energies of hydration: a thermodynamic analysis by ^{1}H NMR, *Biochemistry 35*, 15383−15390.
4. Töhl, J., and Eimer, W. (1997) Interaction of a G-DNA quadruplex with mono- and divalent cations. A force field calculation, *Biophys. Chem. 67*, 177−186.
5. Shafer, R. H. (1998) Stability and structure of model DNA triplexes and quadruplexes and their interactions with small ligands, *Prog. Nucleic Acids Res. Mol. Biol. 50*, 55−94.
6. Kankia, I. B., and Marky, L. A. (2001) Folding of the thrombin aptamer into a G-Quadruplex with Sr^{2+}: stability, heat, and hydration, *J. Am. Chem. Soc. 123*, 10799−10804.
7. Phillips, K., Dauter, Z., Murchie, A. I. H., Lilley, D. M. J., and Luisi, B. (1997) The crystal structure of a parallel-stranded guanine tetraplex at 0.95 Å resolution, *J. Mol. Biol. 273*, 171−182.
8. O'Reilly, M., Teichmann, S. A., and Rhodes, D. (1999) Telomerases, *Curr. Opin. Struct. Biol. 9*, 56−65.
9. Ishikawa, F. (1997) Telomere crisis, the driving force in cancer cell evolution, *Biochem. Biophys. Res. Commun. 230*, 1−6.
10. Hahn, W. C., Counter, C. M., Lunderberg, A. S., Beijersbergen, R. L., Brooks, M. W., and Weinberg, R. A. (1999) Creation of human tumour cells with defined genetic elements, *Nature 400*, 464−468.
11. Hahn, W. C., Stewart, S. A., Brooks, M. W., York, S. G., Eaton, E., Kurachi, A., Beijersbergen, R. L., Knoll, J. H. M., Meyerson, M., and Weinberg, R. A. (1999) Inhibition of telomerase limits the growth of human cancer cells, *Nat. Med. 5*, 1164−1170.
12. Zhang, X., Mar, V., Zhou, W., Harrington, L., and Robinson, M. O. (1999) Telomere shortening and apoptosis in telomerase-inhibited human cells, *Genes Dev. 13*, 2388−2399.
13. Herbert, B., Pitts, A. E., Baker, S. I., Hamilton, S. E., Wright, W. E., Shay, J. W., and Corey, D. R. (1999) Inhibition of human telomerase in immortal human cells leads to progressive telomere shortening and cell death, *Proc. Natl. Acad. Sci. U.S.A. 96*, 14276−14281.
14. Kerwin, S. M. (2000) G-quadruplex DNA as a target for drug design, *Curr. Pharm. Des. 6*, 441−471.
15. Wyatt, J. R., Vickers, T. A., Roberson, J. L., Buckheit, R. W., Jr, Klimkait, T., DeBaets, E., Davis, P. W., Rayner, B., Imbach, J. L., and Ecker, D. J. (1994) Combinatorially selected guanosine-quartet structure is a potent inhibitor of human immunodeficiency virus envelope-mediated cell fusion, *Proc. Natl. Acad. Sci. U.S.A. 91*, 1356−1360.
16. He, G. X., KrawczyK, S. H., Swaminathan, S., Shea, R. G., Dougherty, J. P., Terhorst, T., Law, V. S., Griffin, L. C., Coutrè, S., and Bischofberger, N. (1998) N2- and C8-substitued oligodeoxynucleotides with enhanced thrombin inhibitory activity in vitro and in vivo, *J. Med. Chem. 41*, 2234−2242.
17. Jing, N., De Clercq, E., Rando, R. F., Pallansch, L., Lackman-Smith, C., Lee, S., and Hogan, M. E. (2000) Stability-activity relationships of a family of G-tetrad forming oligonucleotides as potent HIV inhibitors. A basis for anti-HIV drug design, *J. Biol. Chem. 275*, 3421−3430.
18. Hardin, C. C., Perry, A. G., and White, K. (2001) Thermodynamic and kinetic characterization of the dissociation and assembly of quadruplex nucleic acids, *Biopolymers 56*, 147−194.
19. Mergny, J. L., Phan, A.-T., and Lacroix, L. (1998) Following G-quartet formation by UV-spectroscopy, *FEBS Lett. 435*, 74−78.
20. Hardin, C. C., Corregan, M. J., Lieberman, D. V., and Braun, A. B., II (1997) Allosteric interactions between DNA strands and monovalent cations in DNA quadruplex assembly: thermodynamic evidence for three linked association pathways, *Biochemistry 36*, 15428−15450.
21. Williamson, J. R. (1994) G-quartet structures in telomeric DNA, *Annu. Rev. Biophys. Biomol. Struct. 23*, 703−730.
22. Smith, F. W., and Feigon, J. (1992) Quadruplex structure of Oxytricha telomeric DNA oligonucleotides, *Nature 356*, 164−168.
23. Schultze, P., Flint, W. S., and Feigon, J. (1994) Refined solution structure of the dimeric quadruplex formed from the Oxytricha telomeric oligonucleotide d($G_4T_4G_4$), *Structure 2*, 221−233.
24. Randazzo, A., Galeone, A., Esposito, V., Varra, M., and Mayol, L. (2002) Interaction of Distamycin A and Netropsin with quadruplex and duplex structures: a comparative ^{1}H NMR study, *Nucleosides Nucleotides 21*, 535−545.

25. Wang, K. Y., McCurdy, S., Shea, R. G., Swaminathan, S., and Bolton, P. H. (1993) A DNA aptamer which binds to and inhibits thrombin exhibits a new structural motif for DNA, *Biochemistry 32*, 1899−1904.
26. Schultze, P., Macaya, R. F., and Feigon, J. (1994) Three-dimensional solution structure of the thrombin-binding DNA aptamer d(GGTTGGTGTGGTTGG), *J. Mol. Biol. 235*, 1532−1547.
27. Cantor, C. R., Warshow, M. M., and Shapiro, H. (1970) Oligonucleotide interactions. Circular dichroism studies of the conformation of deoxyoligonucleotides, *Biopolymers 9*, 1059−1077.
28. Barone, G., Del Vecchio, P., Fessas, D., Giancola, C., and Graziano, G. (1993) Theseus: a new software package for the handling and analysis of thermal denaturation data of biological macromolecules, *J. Therm. Anal. 39*, 2779−2790.
29. Freire, E., and Biltonen, R. L. (1978) Statistical mechanical deconvolution of thermal transitions in macromolecules. I. theory and application to homogeneus systems, *Biopolymers 17*, 463−479.
30. Aboul-ela, F., Murchie, A. I. H., and Lilley, D. M. J. (1992) NMR study of parallel-stranded tetraplex formation by the hexadeoxynucleotide d(TG_4T), *Nature 360*, 280−282.
31. Laughlan, G., Murchie, A. I. H., Noman. D. G., Moore, M. H., Moody, P. C. E., Lilley, D. M. J., and Luisi, B. (1994) The high-resolution crystal structure of a parallel-stranded guanine tetraplex, *Science 265*, 520−524.
32. Spackova, N., Berger, I., and Sponer, J. (1999) Nanosecond molecular dynamics simulations of parallel and antiparallel guanine quadruplex DNA molecules, *J. Am. Chem. Soc. 121*, 5519−5234.
33. Chawdhury, S., and Bansal, M. (2001) G-quadruplex structure can be stable with only some coordination sites being occupied by cations: a six-nanosecond molecular dynamics study, *J. Phys. Chem. 105*, 7575−7578.
34. Spackova, N., Berger, I., and Sponer, J. (2001) Structural dynamics and cation interactions of DNA quadruplex molecules containing mixed guanine/cytosine quartets revealed by large-scale MD simulations, *J. Am. Chem. Soc. 123*, 3295−3307.
35. Kang, C., Zhang, X., Ratliff, R., Moyzis, R., and Rich, A. (1992) Crystal structure of four-stranded Oxytricha telomeric DNA, *Nature 356*, 126−131.
36. Jorgensen, W. L., Chandrasekhar, J., Madura, J. D., Impey, R. W., and Klein, M. L. (1983) Comparison of the simple potential function for simulating liquid water, *J. Chem. Phys. 79*, 926−935.
37. Cornell, W. D., Cieplack, P., Bayly, C. I., Gould, I. R., Merz, K. M., Ferguson, D. M., Spellmeyer, D. C., Fox, T., Caldwell, J. W., and Kollman, P. A. (1995) A second generation force field for the simulation of proteins, nucleic acids and organic molecules, *J. Am. Chem. Soc. 117*, 5179−5197.
38. Wyatt, R. J., Davis, P. W., and Freier, S. M. (1996) Kinetic of G-quartet-mediated tetramer formation, *Biochemistry 35*, 8002−8008.
39. Petraccone, L., Erra, E., Nasti, L., Galeone, A., Randazzo, A., Mayol, L., Barone, G., and Giancola, C. (2002) Effect a modified thymine on the structure and stability of $[d(TGGGT)]_4$ quadruplex, *Int. J. Biol. Macromol. 31*, 131−137.
40. Lu, M., Guo, Q., and Kallenbach, N. R. (1993) Thermodynamic of G-tetraplex formation by telomeric DNAs, *Biochemistry 32*, 598−601.
41. Guo, Q., Lu, M., and Kallanbach, N. R. (1993) Effect of thymine tract length on the structure and stability of a model telomeric sequences, *Biochemistry 32*, 3596−3603.
42. Smirnov, I., and Shafer, R. H. (2000) Effect of loop sequence and size on DNA aptamer stability, *Biochemistry 39*, 1462−1468.
43. Marky, L. A., and Breslauer, K. J. (1987) Calculating thermodynamic data for transitions of any molecularity from equilibrium melting curves, *Biopolymers 26*, 1601−1620.
44. Jin, R., Gaffney, B. L., Wang, C., Jones, R. A., and Breslauer, K. J. (1992) Thermodynamics and structures of a DNA tetraplex: a spectroscopic and calorimetric study of the tetramolecular complexes of d(TG_3T) and d($TG_3T_2G_3T$), *Proc. Natl. Acad. Sci. U.S.A. 89*, 8832−8836.
45. Breslauer, K. J., Frank, R., Blocker, H., and Marky, L. A. (1986) Predicting DNA duplex stability from the base sequence, *Proc. Natl. Acad. Sci. U.S.A. 83*, 3746−3750.
46. SantaLucia, J., Jr. (1998) A unified view of polymer, dumbbell, and oligonucleotide DNA nearest-neighbor thermodynamics, *Proc. Natl. Acad. Sci. U.S.A. 95*, 1460−1465.
47. Sugimoto, N., Nakano, S., Yoneyama, M., and Honda, K. (1996) Improved thermodynamic parameters and helix initiation factor to predict stability of DNA duplexes, *Nucleic Acids Res. 24*, 4501−4505.
48. Pilch, D. S., Plum, G. E., and Breslauer, K. R. (1995) The thermodynamics of DNA structures that contain lesions or guanine tetrads, *Curr. Opin. Struct. Biol. 5*, 334−342.
49. Simmonsson, T., Pecinka, P., and Kubista, M. (1998) DNA tetraplex formation in the control region of c-myc, *Nucleic Acids Res.* 26, 1167−1172.

BI0300985